IEEE Access
Multidisciplinary | Rapid Review | Open Access Journal

Received 17 July 2024, accepted 6 August 2024, date of publication 12 August 2024, date of current version 21 August 2024.

Digital Object Identifier 10.1109/ACCESS.2024.3441840

TOPICAL REVIEW

Advancements in Neural Recording Circuits: Review of Nerve Biopotentials, and Neural Recording Circuit Architectures

MALAK MNEIMNEH[1], NASIR QUADIR[2], AND LUTFI ALBASHA[2], (Senior Member, IEEE)
[1]Biomedical Engineering Program, American University of Sharjah, Sharjah, United Arab Emirates
[2]Electrical Engineering Department, American University of Sharjah, Sharjah, United Arab Emirates

Corresponding author: Malak Mneimneh (g00098922@aus.edu)

This work was supported in part by American University of Sharjah under Grant FRG23-C-E08, and in part by the Open Access Program from American University of Sharjah.

ABSTRACT Peripheral nerve injuries pose significant health challenges leading to loss of motor control and sensation. These injuries can result from trauma, surgery, tumors, and neurological disorders. Peripheral nerve injuries mainly lead to paralysis such as facial paralysis. Patients with facial paralysis often face loss of facial expression control affecting their quality of life. Research studies have explored peripheral nerve recording to address these challenges, aiming to understand nerve impulses and develop effective neural interfaces for functional restoration. Neural amplifier chips characterized by low noise, high gain, and small size have been integrated with nerve cuff electrodes to capture neural signals efficiently. This paper reviews the applications of cuff electrodes simulating the facial nerve for facial muscle contractions and various neural recording system architectures interfaced with a peripheral nerve cuff electrode. Diverse types of cuff electrodes and their configuration have been drawn pointing out their advantages and limitations. Neural amplifier topologies susceptible to neural recording are outlined with their main characteristics including noise, speed, and power consumption relative to their general architectures.

INDEX TERMS Analog-front end amplifiers, CMOS, electrical neural recording (ENG), facial paralysis, low-noise, low-power, neural amplifiers, nerve cuff electrodes, operational transconductance amplifiers (OTA), peripheral nerve injuries.

I. INTRODUCTION

Peripheral nerve injuries represent the damage of one or more peripheral nerves mostly triggered by trauma with an incident rate of 1.46% to 2.8% notably affecting the upper limbs [1]. Facial paralysis is one of the cases that results from a severed nerve or injury posing a significant clinical and public health challenge [2]. Facial nerve paralysis causes a gradual weakening of facial muscle eventually transforming into scar tissue [3]. Around 0.5 to 5% of patients face facial nerve injuries due to surgeries such as parotidectomy [4]. Neurological disorders like Bell's palsy disease are responsible for 60 to 75% of all cases of facial paralysis [5]. Identifying the reason for Bell's palsy disease remains unknown; however, the effect of this disease represents nerve inflammation characterized by localized swelling, loss of myelination, and reduced blood flow [5]. Other causes of facial paralysis are tumors, such as acoustic neuromas [6]. Restoring connectivity of the facial nerve is complex and requires precise techniques to ensure proper communication. Several treatments exist for chronic facial nerve injuries including surgical repair, nerve grafting, nerve transfer, medications, physical therapies, and electrical stimulation; however, full restoration of the nerve is not quite assembled yet [7], [8]. According to Abiri et al., 10 to 15 % of surgical interventions fail to address more complex facial issues [6]. On the other hand, recent advancements in transcutaneous electrical simulations can be used as a treatment for preventing facial muscle weakening

The associate editor coordinating the review of this manuscript and approving it for publication was Nagendra Prasad Pathak.

by transmitting electric biphasic pulses toward the targeted area [2]. Despite the increased interest in that field, only a few review papers studied facial nerve recording and stimulation via neuroprosthetic circuits.

Implanting cuff electrodes around the proximity of the severed or injured nerve for directly detecting action potentials and simulating it is considered one of the new fields for treating facial nerve paralysis with a long-life span and minimal patient compliance. Detecting nerve signals and simulating the nerve with an effective current amplitude while preventing the destruction of the nerve is considered extremely critical [9]. Neurotechnology and IC designs emerged as tools for replacing pharmacological treatments through integrating various devices, circuit techniques, and conventional devices either in the PNS or CNS for effectively providing therapeutic outcomes while preventing side effects associated with drug intake [10], [11], [12]. Bidirectional neural recording technologies have been currently studied requiring novelty in fabrication for simultaneous stimulation and recording [13]. This has been demonstrated through conventional closed-loop systems or AI integration [13]. Several studies have been interested in integrating implantable neural recording circuits for processing nerve signals through assessing several configurations of nerve cuff electrodes with neural amplifiers [14]. Small neural amplifier chips of low noise, low power, high gain, and high common mode rejection are essential for accurately detecting nerve signals in neuroprosthetic applications. Hence, this review aims to present a survey of neural recording circuit architectures interfaced with nerve cuff electrodes for further answering the following research questions: ''What type of electrode configurations are used with the neural preamplifier?'' and ''What is the output impedance obtained from the nerve cuff electrode recording and does it match the input impedance of the front-end amplifier? Also '' What are the common topologies used for front-end amplifiers?'' Overall, this review is essential to address the gap in current treatments for peripheral nerve injuries more specifically for facial nerve injuries, through improving the integration of neuroprosthetic devices with the nervous system. It outlines the overall neuroprosthetic setups and their communication systems addressing the importance of neural recording circuits and their different architectures. The rest of this article is organized as follows: Section II categorized nerve biopotentials and the main impact of neural recording circuits for treating peripheral nerve injuries. Section III mainly presents different types of cuff electrodes used for implantation indicating their high compatibility and life span. Section IV discusses the configurations of cuff electrodes with neural amplifiers and their electric and ionic behavior necessary for obtaining a high signal-to-noise ratio while minimizing myoelectric interference. Consequently, section V provides the neural recording architectures for filtering out nerve signals along with the communication systems and power supply requirements. Section VI focuses on neural amplifier topologies indicating their advantage in signal acquisition and amplifying the weak neural signal with minimal noise. Section VII summarizes applications used for peripheral nerve recording and section VIII highlights the challenges of peripheral neural recording.

II. PRINCIPLES OF NERVE COMMUNICATION

Neurons communicate through electrical signals via nerve biopotentials categorized as resting and action potentials [15]. The nerve transmission process relies on the potential difference between the extracellular and intracellular membranes [15]. At resting potential, neurons typically maintain a negative membrane potential of -70 mV, with positive ions (sodium Na+, chloride Cl-, and calcium Ca2+) outside and negative ions (potassium K+) inside [16]. Resting potentials are essential for generating an action potential by establishing an electrochemical gradient leading to membrane potential shifting [15], [17]. It is known as the baseline of the electrical charge of a neuron where the signal is not transmitted. The first stage involves the neuron receiving a signal at the neuron's dendrites, branched extensions from the cell body, detecting neurotransmitters released by neighboring neurons [16]. This detection leads to the generation of graded potentials such as excitatory postsynaptic potential (EPSPs) or inhibitory postsynaptic potential (IPSPs), depending on the type of signal received [17]. These graded potentials are mainly integrated at the axon hillock near the cell body region [16], [18]. Once the stimulus receives a threshold (-55 mV), an action potential is triggered, leading to the propagation of impulse along the axon [15], [16]. Thus, action potentials are rapidly causing a transient change in the neuron's membrane potential where voltage-gated sodium channels open allowing sodium ions to enter the potassium ions' exit [15]. This will cause membrane depolarization of -70 mV and will facilitate action potential propagation [16], [17]. As action potential propagates along the axon, sodium gates open sequentially at nodes of Ranvier, found between segments of the myelin sheath ensuring maintenance of signal amplitude and accelerating transmission [16], [18]. The second stage involves the action potential reaching a peak with potassium ions rushing out of the neuron causing repolarization of the membrane [15]. However, to restore the original ion concentration of Na+ and K+, Adenosine triphosphate ATP is required [15]. Consequently, hyperpolarization occurs due to leaky potassium channels, making the membrane more negative compared to the resting potential ~ -75 mV and eventually restoring the initial configuration [15]. Once the action potential reaches the axon terminal, the voltage-gated channels of Ca2+ open causing an influx and triggering the release of neurotransmitters that are stored in the synaptic vesicles [15]. Exocytosis will occur where neurotransmitters bound with the vesicles will be released in the synaptic cleft and eventually bind with the receptors at the postsynaptic membrane, potentially leading to the initiation of new action potential [15], [16]. The bounded neurotransmitter will either depolarize or hyperpolarize the membrane depending on its excitatory or inhibitory nature [17], [18].

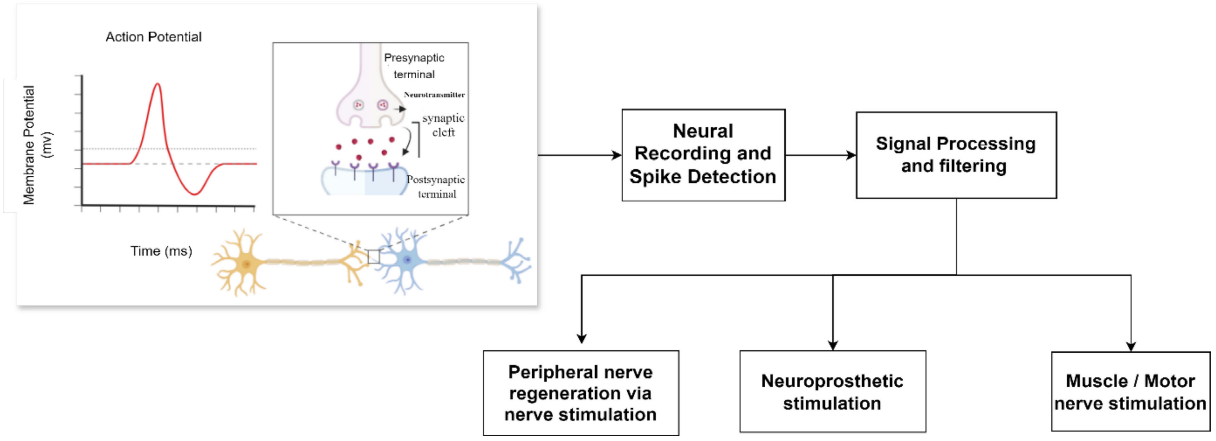

FIGURE 1. Mechanism of neuronal action potential and transmission to the neural recoding circuit for signal processing in neuroprosthetic.

The generated weak electric signal propagated along the axon usually of an amplitude (10 μVpp) can be recorded for signal processing and neuroprosthetic device stimulation through a neural recording interface [19]. More specifically, the generated nerve biopotential represented as the input will be detected by the sensors like electromyography electrodes (EMG) and the analog front-end amplifier, transmitted to the processor enabling natural control of the prosthesis [20], [21]. Advanced neuroprosthesis recently relies on restoring the motor or sensory function by directly integrating it with the nervous system using sensors and machine learning algorithms for detecting gait phases like the lower limb [20]. Inertial measurement units along with EMG electrodes are types of motion sensors that collect data on movement, and muscle activity and transmit it to machine learning algorithms like artificial neural networks and convolutional neural networks for categorizing it into appropriate gait phases [20]. Hence, recording high-quality nerve signals with minimal noise, and signal distortion is essential for further understanding the function and disruption of the nervous system [21]. Furthermore, encapsulating the nerve with scaffolds and stimulating it can enhance the regeneration process and repair of the injured peripheral nerve [22]. A neural recording circuit offers real-time feedback on the generation process, ensuring the effectiveness of different materials and designs in promoting nerve growth and function [23]. A study by Yan et al. developed a decellularized extracellular matrix (dECM) obtained from porcine Achilles tendon tissue, which was doped in a conductive hydrogel material promoting peripheral nerve regeneration [24]. The study showed that ECM-PAM-G hydrogel exhibited electrical conductivity in the neural tissue range, suitable for effective signal transduction between the neural tissues and the recording devices [24]. Upon conducting an invivo study where the conduit was placed between the gaps of the severed sciatic nerve, a neural recording assessment was conducted post-implantation where a stimulus was induced within an intensity of 0.7 mA for 5ms at the proximal and distal ends of the graft site [24]. As a result, the neural electrodes placed on the triceps detected the compound action potential (CMAP) of the triceps muscle which was beneficial to calculating the motor nerve conduction velocity (MNCV) concerning the time delay of the stimulus-induced indicating the success of nerve regeneration in which it varied between different types of nerve guidance conduit [24]. The percentage amplitude of the CMAP and MNCV measured via the neural recording circuits was beneficial for indicating the degree of nerve regeneration and function recovery [24]. Another study done by Song et al., fabricated and tested a dual-functional optical nerve cuff electrode for stimulating and monitoring neural activity specifically for the sciatic nerve [25]. The optical cuff electrode of a bipolar configuration was constructed from polydimethylsiloxane characterized for its compatibility and flexibility as well as enhancing reflection of the light back towards the nerve for effective optical stimulation within a threshold of 2.05 mW/mm^2 [25]. The bipolar electrodes were also of a platinum material characterized by its high conductivity for efficient neural recording and connected to an amplifier detecting a sine wave signal of 8 μV with minimal distortion and artifacts from the optical stimulation [25]. Eventually, neural recording verified the dual function of the cuff electrode for monitoring and stimulating via optical stimulation instead of electrical stimulation in favor of minimizing the electric stimulation interference as well as effectively reflecting the muscle activity for reliable measurement of neuromodulation [25]. Figure 1 represents the nerve biopotential generated between the nerves and the main effect of the neural recording circuit.

III. NERVE CUFF ELECTRODES

Nerve cuff electrodes are categorized as extra neural surface electrodes encapsulated with silicone materials. Electrodes are often platinum materials characterized by high compatibility, durability, and conductivity [26]. An extra-neural cuff electrode wraps around the nerve causing restriction of the extra-cellular space and creating a high resistance area for

TABLE 1. Description of each peripheral nerve interface type and their respective features.

Types of the Cuff Electrode				
Characteristics	Cylindrical Cuff	Split Ring	Flat Interface	Self-Sizing Spiral Cuff
Electrode Arrangement	Monopolar, Bipolar, Tripolar	Flat Ring Splits for multiple Electrodes	Flattened cuff with multiple electrodes	Multiple spiral arrangements of electrodes
Interface	Wrapped around the epineurium nerve layer	Wrapped around the epineurium nerve layer	Placed in contact with the nerve (flatten the nerve)	Adapts to the shape of the nerve and inner edge (penetrates the epineurium)
Advantages	Stable interface for recording and simulation Long term stability	Easy for placement and removal (adjust to nerve diameter)	Increases proximity to fascicles, enhancing spatial resolution	It provides a secure connection between the electrode and

which the nerve signal will pass through [27]. The detected electrical signals result from the summation of electrical activity from multiple nearby nerve fibers [28]. Hence, cuff electrodes could be used as an interface between the nerve and the neural recording chip amplifier for detecting nerve signals and processing them. There exist several types of different biopotential electrodes each classified based on their design and surface area for maximal recording [29].

Several aspects contribute to the morphological properties subjected to the cuff electrode design depending on the targeted nerve location. These properties vary based on the number of contacts, shapes, materials, and sizes [29]. Such types of cuff electrodes are split ring electrodes, a flat ring that is split at one side, allowing it to be placed around the nerve [28]. The electrodes are either placed in a concentric or longitudinal pattern [30]. The encapsulated electrode should have a slightly wider diameter around the nerve ensuring effective recording and stimulation with minimal damage to the nerve [30]. A flat interface (FINE) is another type of electrode that provokes the nerve to flatten as well as achieve greater proximity to the fascicles increasing the spatial resolution [28]. On the other hand, spiral cuff electrodes are embedded with multiple contacts and characterized by a self-curling insulation material allowing more self-adapting and flexibility around the injured nerve [30]. A self-sizing spiral cuff electrode design offers a safer interface than rigid cuffs because of their ability to adapt to different nerve diameters [29]. Table 1 summarizes different types of electrodes including their characteristics.

IV. CUFF ELECTRODES CONFIGURATIONS

Cuff electrodes can enhance neural recording by reducing the volume of tissue in which ENG signals travel, thereby increasing the detection of the action potentials [31]. Cuff electrodes are often designed as longitudinal shapes with circumferential contacts arranged parallelly [29]. The contact electrodes are mainly configured in either monopolar, bipolar, or tripolar manner with the front-end neural amplifiers [29]. Only a few papers have established the recorded signals detected by the cuff electrodes compared to the stimulation applications of peripheral nerves.

A monopolar cuff electrode is represented by one electrode placed near the responsive tissue area known as the positive terminal connected to the positive terminal of the preamplifier relative to a common reference electrode placed outside the cuff [32]. This type of recording for peripheral nerves is commonly sufficient for an ideal-noise-free case [32]. The monopolar electrode is placed at the center of the cuff to increase the recorded neural signal. Despite its simplicity, the monopolar electrode is not ideal for use because it has an imbalance in impedance between the recording and the reference electrodes. This ultimately causes EMG interference that the amplifier can't fully filter out. Another issue is that it can lead to bidirectional action potentials, causing uncontrolled depolarization [33].

A bipolar cuff has two electrodes distinct from each other. The neural recorded signal is obtained based on the differential output between the two electrodes and the low-impedance reference electrode. However, the bipolar electrode can also yield a bidirectional action potential due to forming a virtual cathode near the anodic side causing a cancellation effect [33]. Increasing the gap between the two electrodes allows obtaining a higher recorded signal strength. Placing the electrodes at the outer extremities of the nerve leads to a decrease in the neural signal's strength [28], [29], [31]. The tripolar cuff electrode is the most common configuration interfaced with the preamplifier. Tripolar electrodes are placed equidistant from each other in which the recorded signal output is obtained between the center and outer electrodes [34]. Similar, to bipolar, the further the electrodes are placed the greater the potential difference indicating better signal quality [29]. An advantage of the tripolar cuff electrode in comparison with the other types of configurations is that shortening the two outer electrodes allows removing external noise [35]. Hence, interfacing the cuff electrode with a suitable differential amplifier can minimize the interference and give a reliable nerve signal such configuration can be attained by the Quasi-tripolar and true-tripolar

electrodes [34]. Quasi-tripolar electrode represents an additional two equidistant shorted electrodes at the central causing an increase in signal-to-noise ratio by 11 % [36]. As for the true-tripolar electrodes, the configuration is done by adding two output amplifiers after amplifying the central electrode causing an improvement of signal-to-noise ratio by 10 % [37]. Other configurations are done for removing noise either by adding two shorted electrodes at extremities known as screened tripolar or by adding an external conductive shield encapsulating the entire cuff's external surface [35]. A summary of the nerve cuff electrode configurations and types is present in Figure 2.

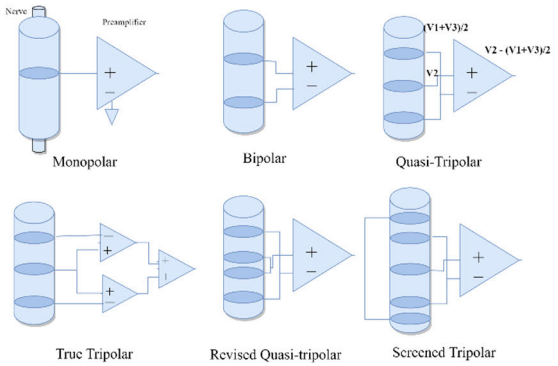

FIGURE 2. Nerve cuff electrode configurations for extra neural recording.

A. ELECTRODE CIRCUIT MODELING

In the field of neuroprosthetic, nerve cuff electrodes' electric circuit behavior can be represented in the form of impedance modeling of the electrode-electrolyte interface [38]. This type of model representation allows suitable measurement of the output impedance of the cuff electrodes making it suitable to match the input impedance of neural amplifiers preventing any voltage drop. Two common models for representing the electrode electrolyte-electrolyte impedance for a broader frequency range are the Randle and Cole circuit models shown in Figure 3 [38], [39], [40]. Randles model, established in 1947, is composed of an access resistance (Rs), and active electrolyte resistance which varies based on several factors such as the electrode material, and tissue encapsulation connected in series with a double layer capacitance Cdl and in parallel with the impedance of a faradic reaction [40]. Faradic reactions occurring at the electrode-electrolyte interface are represented as Rct known as the charge transfer resistance in series with Warburg impedance (Zw) reflecting the ion diffusion at the interface and impacting frequency-dependent behavior [39], [40]. In the Randle model, at higher frequencies, the access resistance dominates due to the capacitance acting as short. Opposingly, at lower frequencies, the Zw takes over indicating ion diffusion from the electrolyte towards the interface [39], [40]. Cole's model established in 1940 replaced the double capacitance Cdl with a new impedance known as constant phase element CPE that represents both the double layer capacitance considering surface irregularities and chemical reaction at the interface [38]. The Cole equivalent circuit model is represented as a parallel network of the ZCPE parallel to Rct, and an active electrolyte resistance (Racces) is represented in the following equation [38].

$$Z = R\infty + \frac{(R0 - R\infty)}{1 + (j\omega/\omega 0)\hat{}\alpha} \tag{1}$$

Equation 1 represents the total impedance at the interface where $R\infty$ is dominant at higher frequencies and resistance R0 would be observed at lower frequencies [38]. The impedance Z varies concerning angular frequency (ω) [38]. As for the constant (α) it represents the shape of the impedance curve transitioning between the two resistive components as frequency changes [38]. Thus, this equation demonstrates how the impedance of the cuff electrode varies with different signal frequencies depending on the nerve or electric signals passing through it either fast or slow. The constant phase element (ZCPE) has a magnitude that remains constant regardless of the electric signal frequency passing through. The phase element on the other hand changes where when $\alpha = 1$, the CPE behaves purely like a capacitor, and when $\alpha = 0$, the CPE behaves purely like a resistor [38]. For ideally polarizable electrodes typically fall between 0.5 and 1, indicating a mixed behavior between purely capacitive and purely resistive [38]. In the Cole model, the CPE has a consistent behavior across decreasing frequency due to excluding the diffusion process making it suitable to represent the consistent polarization impedance behavior of cuff electrodes regardless of the frequency.

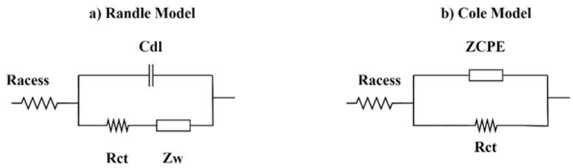

FIGURE 3. (a) Randle equivalent circuit model and (b) Cole circuit model [38], [39], [40].

B. NERVE CUFF ELECTRODES IN FACIAL PROSTHESIS

Several research studies have examined the efficacy of nerve cuff electrodes in stimulating facial muscles, yet there are limited studies done on recording nerve signals from injured facial nerves. Multichannel dual-cuff electrodes were used for the stimulation of the injured facial nerves [6]. Each cuff had an inner diameter of 1.5 mm with two separate rings of four rectangular tripolar platinum contacts arranged concentrically every 90 degrees, which allowed for proper placement and contact with the facial nerve [6]. Based on the average reported value of charge injection capacity (CIC) for platinum electrodes the maximum current intensity was 1.22 mA [6]. The electrode impedance was measured to be 0.5 kΩ at 1000 Hz, ensuring proper electrical conductivity [6]. These specifications of the MCE system were chosen to ensure effective and selective activation of individual facial muscles such as levator, nasalis, and oculi muscles at low stimulation amplitudes 15 uA while minimizing the potential for current-induced nerve injury [6]. Another study implanted

TABLE 2. Neuroprosthetic devices applications for facial paralysis.

Cuff Type	Characteristics	Target Area	Result	Reference
Dual Cuff Electrode	• 8-channel MCEs, inner diameter of 1.5 mm, • two separate rings of four, 100 × 100 µm rectangular platinum contacts • Arranged concentrically, bipolar stimulation capability	• Main trunk of the FN, dorsal (upper branch) • Ventral (lower branch) rami of the FN	• MCE1 (channels 1-8) stimulation of nasalis and mild-moderate activation of platysma • MCE2 (channels 9–16) selective for levator and oculi.	[6]
Bipolar cuff electrode	Silicon-sheathed nerve cuff with platinum-iridium	• Group 1 a: zygomatic and buccal branch • Group 1 b: Buccal Branch • Neural Blockage: Left buccal branch.	• High prediction compatibility of recorded signal 96% • Blockage of undesirable muscle activation	[41]
Dual Cuff electrode	• 8-channel MCEs, inner diameter of 1.5 mm, • two separate rings of four, 100 × 100 µm rectangular platinum contacts • Arranged concentrically, bipolar stimulation capability	Main Trunk of the Facial Nerve	• Levator and Nasalis muscle activation at 1 mA • Selective Levator muscle activation 0.56 mA	[42]

bipolar nerve cuff electrodes in Wister rats to stimulate injured facial nerves, especially the buccal and zygomatic branched of the facial nerve [41]. The pulse stimulation amplitude ranged between 0.1 to 2 mA within 0.4 msec for an effective stimulation preventing any damage to the nerve [41]. Another study used the same multi-channel dual cuff electrode and simulated it using a fabricated prototype device that can detect and process electromyographic (EMG) input through a portable micro-circuit board [42]. A graded biphasic electrical pulse of a duration of 82 μs per phase was simulated at an intensity of ∼1 mA, ∼0.56 mA, and 0.36 mA allowing the patient to mimic the strength of healthy facial muscles [42]. Table 2 summarizes the setups used in the following facial muscle activation through nerve stimulation.

V. NEURAL RECORDING CIRCUIT ARCHITECTURES

The conventional design of neural recording circuits typically includes a low noise preamplifier(LNA) followed by a bandpass filter. A bandpass filter includes both a high pass filter to eliminate DC offsets in neural signals and prevent recording saturation meanwhile a low pass filter allows capturing local field potentials and improving signal-to-noise ratio by filtering out higher-frequency noise [43]. Multichannel neural recording circuit architectures use multiplexers to direct neural signals to the analog front-end circuit input [44]. The general circuit architectures of multi-channel recording circuits are categorized as a time-division multiplexing system and a frequency-division multiplexing system [44]. TDM system amplifies and transmits multiple neural signals through a single ADC using the time-splitting method. Individual amplifiers and filters are integrated for each electrode and then front-end using a multiplexer [39]. As for the rapid TDM, a back-end multiplexer minimizes chip area [39]. This type of architecture was depicted in a neural prosthetic device to record nerve signals and control urination based on the bladder state [45]. The neural recording circuit architecture exhibited a typical traditional neural recording circuit by implanting a preamplifier module followed by a bandpass filter and 8 AC coupled differential amplifiers connected to an analog time-division multiplexer [45]. The FDM method modulates the signals from each channel to different frequencies and transmits the signals into a single wire toward the LNA and ADC [44]. The neural amplifiers used in the neural recording circuit must be capacitively coupled where the input capacitor Cin is connected to the input of the LNA to block DC offsets allowing only AC neural signals to pass through [43]. In the case of a closed-loop neural recording circuit, a feedback capacitor is integrated to set the gain of the amplifier [43]. Figure 4 summarizes the common neural recording circuit architectures. Hence, the neural recording circuit serves as a setup for neural signal amplifications, detecting weak neural signals and backdrops of high noise. It is considered the front-end signal processing circuit that maintains low noise levels and high input impedance [46].

A. POWER SUPPLY PROTOCOLS

Implantable multichannel neural recording circuits should acquire low power consumption, heat dissipation, and

compact size. The rise temperature limit for commercial implants is between 1-5 °C and requires low power supplies to minimize tissue damage ranging between a few mV and μV aiming to maintain minimal tissue heating and prolong device battery life [14]. A study done by Deshmukh et al. relied on wireless inductive charging via a coil implanted near the recording system and transmitter outside [47]. For small animals, the charging was done via far-field charging by placing a charging cage which freely allows clinical recording and experimentation for the researcher [47]. The energy harvesting system was carefully adjusted via the coil, inductor, and resistance to ensure that the heat dissipated remains below the region of 1.5 degrees Celsius [47]. Another study by ElAnsary et al. integrated a 130 nm CMOS technology that consumes 140 nW power consumption for sciatic peripheral neural recording via 64-channel electrodes [48]. Their power design represented integrating a receiver coil (Rx) on a silicon area of 4.8 mm^2 with a quality factor of 5 and 8 allowing efficient energy storage and wireless power transfer with minimal loss [48]. The transmitter coil is optimized with a radio frequency interrogator ensuring maximum power transmission within a frequency of 60 MHz while abiding with a specific absorption rate and temperature of 1.5 °C [48]. Recently, studies have focused on implanting neuroprosthetic devices or integrated chips without the need for conventional batteries [49]. A recent study done by Shen et al. proposed a battery-free operation system for the neural recording chip by relying on wireless power transmission and passive body channel communication (BCC) eliminating the need for surgeries for battery replacement [49]. The power supply transfers galvanic power through the body's natural conductive pathways including tissues and fluids [49]. The study successfully decreased the power consumption to 30.4 uW leading to minimal heat release [49]. The proposed power supply system relies on generating a 1 MHz signal that penetrates the electrodes placed on the skin surface, creating a voltage across the implanted electrodes [49]. The transferred power will then be converted to DC power ranging between 1.4 to 1.7 V via a rectifier [49], [50], [51]. In neuroprosthetics, the power transfer should also be sufficient for the neurostimulators and processors. Neuromorphic circuits require a range of 10 to 100 μA current consumption to effectively deliver a biphasic current pulse with minimum tissue damage [52]. Overall, neural prosthetic devices are categorized into three main blocks: neural recording circuits, signal processors, and neural stimulators. The system should consume minimal power such that the neural recording circuit can suppress any large stimulation with minimal artifacts by integrating efficient power management mainly via wireless transmission and filtering [53].

B. COMMUNICATION SYSTEM OF NEUROPROSTHETIC

Neuroprosthetic devices emerged as a tool for enhancing neural connectivity and preventing paralysis [54]. It is either categorized as a non-invasive or invasive integrated chip depending on the condition [54]. Usually, upper limb paralysis relies on a non-invasive category allowing control of exoskeletons and other assistive devices. On the other hand, invasive chips are more likely to be used for brain-machine interfaces, pain relief, and regeneration of the severed nerve. Noninvasive technology is more favored since it doesn't require surgical interventions, reduces cost, and increases multitasking [55]. Millimeter waves (MMWs) are one of the techniques recently studied for non-invasively stimulating the nerve providing high specificity and minimal damage [56]. A study done by Song et al. transmitted MMws wave at 60 GHz inducing a stimulus of 13 dB at the auricular branch of the vagus nerve [56]. This type of stimulation has the potential to allow precise neuromodulation therapy with minimal invasiveness by increasing the local field potential (LFP) power in the nucleus [56]. Millimeter waves are electromagnetic waves operating at a frequency range of 30 to 300 GHz which have been increasingly being explored in neural recording circuits either for wireless power transmission or for transmitting large volumes of data [57], [58]. On the other hand, neural implants consist of electrodes for neural detection, a signal processing module to detect neural spikes, and a wireless transmitter to communicate with the stimulator for effectively triggering muscle contraction or blocking a neural response and a power supply unit [59]. Pressure sensors are used in certain prosthetics for allowing movement like hand grasping in which pressure sensors are placed on the fingers triggering the device to generate a movement for holding objects [59]. Biopotential amplifiers are considered the first front-end interface with the cuff electrodes to transmit the ENG signals [59]. A study conducted by Ionescu et al. integrated cuff electrodes with a conventional low-noise pre-amplifier INA118 [59]. The communication system between the detected signal and the processing unit or external device was via Bluetooth Communication module (HC-05) [59]. As for the microcontroller, an Atmega328 controller was used for processing the signal [59]. The circuit was powered via an inductive power supply including a voltage stabilizer, an oscillator, and a coil [59], [60]. While neural acquisition and stimulation have primarily targeted spinal cord injuries, urinary bladder function management, sciatic nerve stimulation, promotion of hand-grasp and ocular stimulations [45], [61], [62], [63], [64], only a few papers have addressed the stimulation of facial nerves targeting the contraction of facial muscles with no neuroprosthesis devices or implantable interface for neural recording. Research studies have either focused on recording EMG signals from the healthy facial side or stimulating and recording facial muscles rather than recording the facial nerve signals to bypass the injury and prevent paralysis or allow sensation, especially in cases of bilateral facial paralysis [41], [42], [65], [66].

Neuroprosthetic systems are subdivided into either open-loop neuromodulation systems, closed-loop, or adaptive systems integrated with AI technology [67]. Unlike a closed loop system, the open loop measures the nerve biopotential signal which triggers a preset stimulation parameter

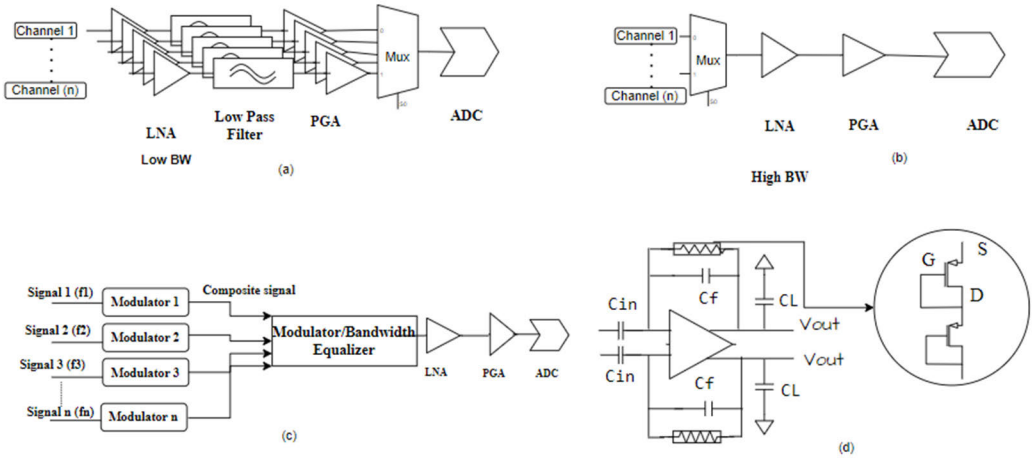

FIGURE 4. Neural recording architecture (a) Time division multiplexer based, (b) Rapid TDM, (c) Frequency division multiplexer, (d) AC coupled amplifier.

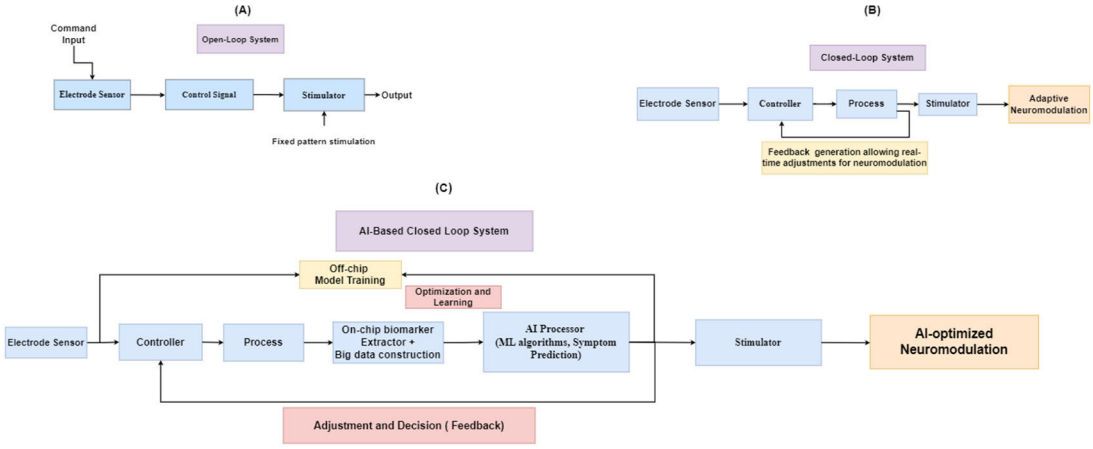

FIGURE 5. Neuromodulation system setups with (a) open loop system, (b) Closed loop system (c) AI Closed- loop system.

TABLE 3. Comparison of parameters between the four OTA topologies.

Topologies	2-stage-Miller OTA	Symmetrical Cascode	Telescopic OTA	Folded Cascode OTA
Gain	High	Medium	Medium	Medium
Speed	Low	Medium	High	High
Output Swing	Highest	Medium	Medium	High
Power	Low	Medium	Medium	Medium
Noise	Low	Medium	Low	Medium

with no response to physiological feedback [67]. Meanwhile, closed-loop systems are considered more advanced indicating more research interest in the field of neuroprosthetics [67]. It incorporates processors and controllers that further offer real-time feedback to adjust the parameters of stimulation [67]. Finally, advanced technologies rely on interfacing AI algorithms for continuous adaptation and optimization of large neural recording sets [67]. Figure 5 represents a comparison of the different system setups. Closed loop systems are more favored than other systems due to their advantages of reducing power consumption and being less complex than AI-integrated systems [68]. An example of an open loop system is a study done by Loi et al., where a tf-Life electrode encapsulated the sciatic nerve and connected

to a neural recording circuit [69]. This recorded signal is filtered out within 800 Hz to 3 KHz and amplified up to 96 dB [69]. The signal is further transmitted to a PC that digitizes the signal and then manually stimulates the nerve within a programmed frequency and amplitude making it an open-loop system with no real-time feedback response [69]. Not only closed-loop systems are used in case of paralysis but also as a therapeutic technique for treating various neuropsychiatric problems [70]. It has lately been used as a treatment for deep brain stimulation and for treating several diseases including Alzheimer's and Parkinson's disease [70]. Closed-loop systems have also been used for treating hypertension by interfacing neural recording circuits with the vagus nerve or via deep brain stimulation [71], [72]. A study done by Shen et al. detected neural signals from the vagus nerve using RHS2116 chip [72]. The detected neural signal is sent wirelessly via Bluetooth into an external mobile application for real-time processing and adjusting the electrical stimulation parameters to achieve therapeutic effects in lowering blood pressure [72]. Closed-loop systems enabled with artificial intelligence networks are designed to automatically detect the neural signal and adjust the stimulation parameters within milliseconds [73]. Machine learning algorithms are typically used as a tool for training the AI system externally using large data sets before integrating it with the closed-loop circuit which would then continue to learn and adapt to the patient's case [73].

VI. NEURAL AMPLIFIER TOPOLOGIES

Front-end operational amplifier designs referred to as operational transconductance amplifiers (OTA) can be integrated using various architectural designs [14]. The OTA is a type of amplifier used in a neural system where unlike the usual amplifiers (OPAMP), it doesn't need a power-consuming output circuit except for the high-resistance pseudo-resistor in its feedback network [74]. OTAs are characterized by their fast speed compared to the conventional low output impedance op-amp and their transconductance tunability (Gm $\alpha\sqrt{2.IBias}$) [75]. In the case of OTA, the process of amplifying the signal utilizes transconductance where the input voltage signal is converted into a current which is further processed. The input referred noise of the OTA arising from thermal and flicker noise of the transistor's channels is managed by adjusting the bias current and gate areas [74]. To minimize the noise and improve efficiency factors like noise efficiency factor NEF and power efficiency factor PEF, the input transistors operate in a weak inversion zone, receiving a significant biasing current. Balancing flicker noise reduction with increased capacitance due to a larger gate area is crucial, requiring careful sizing of the input differential pair [14], [75]. Ng and Xu suggested turning the area of the input differential pairs over the signal bandwidth to minimize the input-referred noise and NEF by adjusting the choice of gate width (W) and length (L) of the input transistors [76]. If the noise is dominant in the operating bandwidth, the gate area should be higher to minimize the input-referred noise. Hence, the transistor width is maintained to ensure a high transconductance, and the gate length is adjusted to achieve a balance between reducing flicker noise and avoiding excessive capacitance [14], [75], [76].

Cascode amplifiers enhance the gain within OTA topologies, specifically designated for low-voltage neural amplifiers such topologies are two-stage Op-Amp (Miller OTA), folded cascode, telescopic cascode amplifier, symmetrical Cascode OTA where each characterized with distinct trade-offs in performance and power consumption (fig. 6) [14], [74], [75], [76], [77]. The 2-stage Miller OTA consists of two stages which are a differential amplifier with an active load and a common-source amplifier with a large Miller capacitor respectively. The first stage allows amplification of the input difference between nerve signals and the second stage provides additional voltage gain [14], [74], [75]. The Miller topology is characterized by allowing high gain and bandwidth making it suitable for detecting peripheral nerve signals [78]. However, it requires a large part of the supply current to maintain stability in their second stages leading to higher NEFs which is undesirable in neural signals [74]. As for symmetrical cascode topology, it uses a cascode configuration with two identical transistors connected in a row. While it's a single-stage amplifier comprising a differential input pair, a cascode stage, and a current mirror, like the 2-stage Miller OTA, it also demands a considerable portion of the supply current, resulting in higher NEFs. [74]. Both telescopic cascode and folded cascode consist of common source stages followed by common gate stages [14], [74], [75]. However, the telescoping cascode OTA is based on a cascode configuration with transistors connected in a row providing high input impedance and low output impedance [76]. Telescoping OTA has the lowest input noise levels compared to the other OTAs. On the other hand, the folded OTA consisted of a common source stage followed by a cascode stage which was then followed by a common gate stage. This topology is preferred for peripheral nerve recording due to providing high output impedance, employing a wide range of input and output common mode swings, and the ability to connect feedback; however, its two-stage design requires more power consumption [14], [74], [75]. The term folded effect is due to using a cascode configuration with two transistors connected in a row. Table 3 outlines the characteristics of each topology.

VII. APPLICATIONS OF PERIPHERAL NERVE RECORDING

Traditional neural amplifiers discussed above may require additional customization to accommodate detecting neural signals effectively. This includes customized amplifier designs, bandwidth constraints, low power, and low noise CMOS amplifiers. Applications presented later are limited to neural amplifiers integrated with cuff electrodes mainly or subjected to peripheral nerve recording specification. Limited research has focused on integrating neural amplifiers for peripheral nerve recording with most of the studies

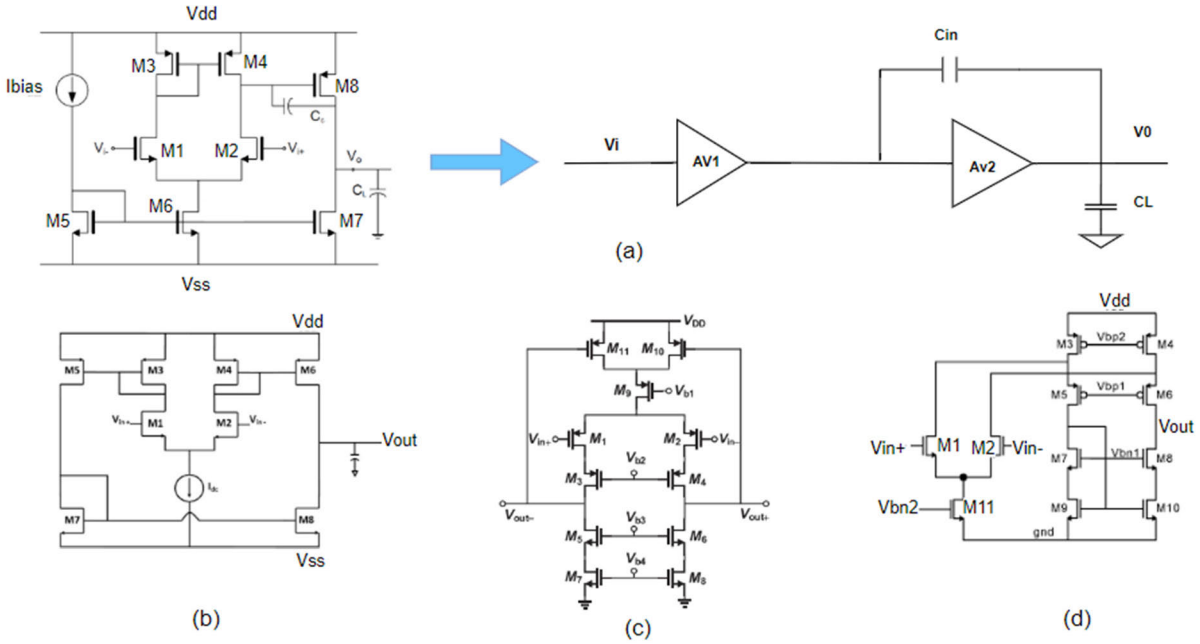

FIGURE 6. (a) 2-Stage Miller OTA and frequency response, (b) Symmetrical cascode OTA, (c) Telescopic OTA, (d) Folded cascode OTA.

focusing on the central nervous system. As for facial nerve recording studies have focused on studying clinical functional electrical stimulation rather than fabricated integrated IC design. A two-stage OTA amplifier was integrated by Naderi et al. suitable for neural amplification [77]. The integrated amplifier does not require any compensation since all nodes were diode-connected except for the output node [77]. The neural amplifier fabrication methods involved rail-to-rail current reuse design facilitating a broader output swing for enhanced suitability in neural signal amplification while maintaining low power and noise compared to conventional amplifiers [77].Another neuroprosthetic device for peripheral nerve recording and stimulation was interfaced with a revised quasi-tripolar cuff electrode targeting the peroneal nerve fabricated by Shon et al. (2018) [62]. The neural architecture implanted was a typical traditional architecture of a preamplifier AC coupling filter with T-network topology, bandpass filter, and ADC [62]. Conventional neural amplifiers were used as an LNA (INA11) as well as a conventional PGA (LTC6911) [62]. The neural amplifier was simulated by inducing a sinusoidal signal, one of peak 1 v and frequency 1.5 KHz which was reduced to 10 mv representing the neural signal while the second signal was a 1 v with 60 Hz testing efficient common-mode voltage [62]. On the other hand, a compact low-noise amplifier fabricated by Liu and Walker for peripheral nerve recording obtained input signals using a Utah Slanted electrode array implanted in a feline sciatic nerve [79]. The integrated amplifier utilized a combination of chopping and switched capacitor (SC) filtering techniques to achieve low noise and area [79]. The chopping method was implemented to reduce flicker noise, while SC filtering allows for low-power and low-pass filtering. The OTA topologies used are based on Miller-neutralization MOS capacitors and folded cascode structures to achieve high gain and flexible common mode levels [79]. A study conducted by Dweiri et al. conducted peripheral nerve recording using a conventional ultra-low noise miniaturized neural amplifier integrated with a Fine nerve cuff electrode at the sciatic nerve [80]. The neural amplifier used consisted of multiple parallel CMOS OTAs connected to each contact (16-contact) of the Fine electrode [80]. The number of OTAs was adjusted using the averaging hardware technique reducing the intrinsic noise of the amplifier. Each contact was connected to the input of eight parallel CMOS OTA which were then averaged in groups of one through eight per contact for comparison [80]. A sacral nerve recording for bladder control has been integrated using a time division multiplexed neural recording circuit architecture fabricated by Wang et al. [45]. The recording circuit contained an 8-channel AC coupled fully differential input preamplifier [45]. The AC-coupled amplifier is an OTA-based amplifier with a T-capacitor feedback network topology [45]. Similarly, a CMOS neural recording amplifier for implanted quasi-tripole electrodes was fabricated by Desmosthenous et al. for peripheral nerve recording aiming to prevent paralysis as well as bladder stimulation [81]. The neural amplifier was designed to neutralize EMG interference using a programmable switched resistor and capacitor. The amplifier used the current feedback technique to achieve a high CMMR above 80 dB [81]. The circuit architecture consisted of two resistive degenerated transconductances, each featuring an isolated local feedback loop. In the input transconductor, the equalization

TABLE 4. Parameters of neural recording amplifiers for peripheral nerve recording.

Parameter	[77]	[62]	[79]	[80]	[45]	[81]
CMOS technology (um)	0.18	-	0.18	-	0.18	0.35
Supply Voltage (V)	1.2	3.3	1.8	3.3 V	1.8	3
Supply current (uA)	-	-	36.8	-	0-500	310
Gain (dB)	39.93	38-123	58	-	80-117 dB	6-47
Operating Bandwidth (HZ-KHz)	0.6-5	237-5478 Hz	476-9.75	700-7	300 -3	100-12
Input referred noise (uVrms)	3	792.47 nV	1.4	<1.5	0.069	0.68
Noise Bandwidth (Hz-KHz)	-	300-5	-	-	-	60 -14.65
NEF	1.68	100	3.45	-	-	4.2
CMRR (dB)	>70 dB	-	55	-	-	99
PSRR (dB)	>80	-	58	-	-	85
Area (mm^2)	0.03	28*33*12	0.034	-	1.6	0.08

of drain currents in the transistor M1 and M2 facilitated the input stage's operation as a unity-gain buffer [81]. Similarly, for the output transconductor, the matching of drains in transistors M1 and M2 ensured that the currents at I1 and I2 be the same at I3 and I4 resulting in output voltage at R2 leading to representing the DC gain of their amplifier as R2/R1. The frequency response characteristics of the circuit were controlled by introducing a dominant pole achieved through R2 in parallel with R1 [81]. Each study represented a unique approach to neural amplification based on the neural signal types. The specs of each peripheral nerve recording application discussed are summarized in Table 4.

VIII. CHALLENGES OF PERIPHERAL NEURAL RECORDING

Despite advances in state-of-the-art technology, fabricating neural recording circuits that can amplify weak neural signals to large amplitudes with minimal distortion remains challenging [74]. Neural signals are of low amplitude which may be lost or hard to be filtered out from external signals like myoelectric interference or flicker and thermal noise originating from the neural amplifier system. [74]. Hence, the input-referred noise of the preamplifier should be less than 10 μV achieving a high gain of up to 60dB [82]. However, ensuring the preamplifier reaches the required noise specs can ultimately consume 30% of the total power of the neural recording circuit which is considered critical for releasing heat especially when integrated near the biological tissues that may cause damage to the interfaced nerve [82]. Another challenge is integrating neural recording circuits of multiple channels with a minimal surface area while maintaining the NEF where larger MOSFETs can reduce flicker noise and improve the transconductance but increase the surface area [82]. Most neural technologies are integrated using 180 nm technology or less posing significant challenges to reaching the required gain (gm) [82], [83]. These scaled MOSFETs are characterized by the short channels effect decreasing the transconductance and increasing the gate current leakage; thus, reducing the efficiency of the circuit [83]. DC-coupled neural amplifiers are a solution for increasing the gain; however, their mid-band gain is highly sensitive causing undesired shifts in the low cut-off frequencies which affects the filtering capabilities of unwanted low-frequency noise [83]. On the other hand, AC-coupled amplifiers suffer from low input impedance capacitance degrading the quality of the neural signals by causing signal attenuation and decreasing SNR [83]. Implantable neural devices are still under clinical studies where there is no further understanding of the communication system between the nerve and the interfaced device in terms of medical view, especially for severed nerves as well as the long-term implantation effect [84]. In terms of electrodes, configuring the electrodes in proximity to the nerve poses significant challenges for scaling multi-electrodes within various neural recording

channels while minimizing the impedance and myoelectric interference as well as constraining the pressure around the nerve for minimal damage [85]. Each cuff electrode should be configured based on the size of the peripheral nerve making it difficult to fabricate a universal cuff electrode that fits patients in different areas [86]. In summary, the implantable neural interface device should be biocompatible, handle a large dynamic range of neural signals simultaneously, small surface area, and suppress stimulation artifacts. allowing safe and reliable long-term usage [69], [84], [87].

IX. CONCLUSION

Past research studies mainly focused on nerve cell physiology and the functionality of peripheral nerve recordings. However, integrating neural recording circuits with single or multi-channel peripheral nerve recording provokes the ability to detect the nerve signal despite any injury allowing processing and sorting. Hence, understanding the frequency bandwidth of nerve signals as well as their amplitudes would pave the way for setting up neural stimulators that will further mimic the nerve pulse signal for different applications. Such applications may be beneficial for either inhibiting or blocking nerve signals such as in case of pain upon setting the pulse within a certain amplitude, time, and frequency range. Other applications would include regenerating the nerve in case of trauma or severed nerve preventing paralysis. Hence, current state-of-the-art technologies provide great advances in spinal cord injuries, hand grasping, and bladder contraction in the case of diabetes.

ABBREVIATIONS

The abbreviations used in the manuscript are arranged alphabetically as follows:

ADC	Analog-to-Digital Converter.
AC	Alternating Current.
BCC	Body Channel Communication.
Cin	Input Capacitor.
CMOS	Complementary Metal-Oxide-Semiconductor.
CMRR	Common-Mode Rejection Ratio.
DC	Direct Current.
EMG	Electromyography.
FDM	Frequency-Division Multiplexing.
GHz	Gigahertz.
LFP	Local Field Potential.
LNA	Low Noise Amplifier.
MHz	Megahertz.
NEF	Noise Efficiency Factor.
OTA	Operational Transconductance Amplifier.
PCB	Printed Circuit Board.
RMS	Root Mean Square.
SNR	Signal-to-Noise Ratio.
TDM	Time-Division Multiplexing.

REFERENCES

[1] A. Lavorato, G. Aruta, R. De Marco, P. Zeppa, P. Titolo, M. R. Colonna, M. Galeano, A. L. Costa, F. Vincitorio, D. Garbossa, and B. Battiston, "Traumatic peripheral nerve injuries: A classification proposal," *J. Orthopaedics Traumatology*, vol. 24, no. 1, p. 20, May 2023, doi: 10.1186/s10195-023-00695-6.

[2] M. Modrak, M. A. H. Talukder, K. Gurgenashvili, M. Noble, and J. C. Elfar, "Peripheral nerve injury and myelination: Potential therapeutic strategies," *J. Neurosci. Res.*, vol. 98, no. 5, pp. 780–795, May 2020.

[3] R. K. Mistry, M. H. Hohman, and A. A. Al-Sayed, *Facial Nerve Trauma*. Treasure Island, FL, USA: StatPearls Publishing LLC, 2023.

[4] C. M. Klein, "Diseases of the seventh cranial nerve," in *Peripheral Neuropathy*, 4th ed., P. J. Dyck and P. K. Thomas, Eds., Philadelphia, PA, USA: W.B. Saunders, 2005, pp. 1219–1252. [Online]. Available: https://www.sciencedirect.com/science/article/pii/B9780721694917500533

[5] A. Singh and P. Deshmukh, "Bell's palsy: A review," *Cureus*, vol. 14, no. 10, 2022, Art. no. e30186.

[6] A. Abiri, S. Chau, N. R. James, K. Goshtasbi, J. L. Birkenbeuel, R. Sahyouni, R. Edwards, H. R. Djalilian, and H. W. Lin, "Selective neural electrical stimulation of an injured facial nerve using chronically implanted dual cuff electrodes," *Brain Sci.*, vol. 12, no. 11, p. 1457, Oct. 2022.

[7] T. Kornfeld, P. M. Vogt, and C. Radtke, "Nerve grafting for peripheral nerve injuries with extended defect sizes," *Wiener Medizinische Wochenschrift*, vol. 169, nos. 9–10, pp. 240–251, Jun. 2019.

[8] E. Evgeniou, D. N. Mitchell, and S. M. Rozen, "Cross facial nerve grafting for smile restoration: Thoughts on improving graft inset," *Plastic Reconstructive Surg. Global Open*, vol. 10, no. 6, p. e4178, Jun. 2022.

[9] C. Günter, J. Delbeke, and M. Ortiz-Catalan, "Safety of long-term electrical peripheral nerve stimulation: Review of the state of the art," *J. NeuroEng. Rehabil.*, vol. 16, no. 1, p. 13, Dec. 2019, doi: 10.1186/s12984-018-0474-8.

[10] A. Schmid, T. Tokuda, and M.-D. Ker, "Editorial: Microelectronic implants for central and peripheral nervous system: Overview of circuit and system technology," *Frontiers Neurosci.*, vol. 15, Nov. 2021, Art. no. 794944.

[11] H. Chandrakumar and D. Markovic, "A high dynamic-range neural recording chopper amplifier for simultaneous neural recording and stimulation," *IEEE J. Solid-State Circuits*, vol. 52, no. 3, pp. 645–656, Mar. 2017.

[12] T. Stieglitz, "Why neurotechnologies? About the purposes, opportunities and limitations of neurotechnologies in clinical applications," *Neuroethics*, vol. 14, no. 1, pp. 5–16, Apr. 2021, doi: 10.1007/s12152-019-09406-7.

[13] Y. Jung, H. Jeon, T. Lee, H. Y. Seong, C. Park, and M. Je, "Technical review: Neural recording circuits for bidirectional neural interface," in *Proc. IEEE Int. Conf. Consum. Electron.-Asia (ICCE-Asia)*, Jun. 2018, pp. 206–212.

[14] E. Bharucha, H. Sepehrian, and B. Gosselin, "A survey of neural front end amplifiers and their requirements toward practical neural interfaces," *J. Low Power Electron. Appl.*, vol. 4, no. 4, pp. 268–291, Nov. 2014.

[15] J. Feher, "3.3—Propagation of the action potential," in *Quantitative Human Physiology*, 2nd ed., J. Feher, Ed., Boston, MA, USA: Academic, 2017, pp. 280–288. [Online]. Available: https://www.sciencedirect.com/science/article/pii/B9780128008836000252

[16] D. A. McCormick, "Membrane potential and action potential," in *From Molecules to Networks*, 3rd ed., J. H. Byrne, R. Heidelberger and M. N. Waxham, Eds., Boston, MA, USA: Academic, 2014, ch. 12, pp. 351–376. [Online]. Available: https://www.sciencedirect.com/science/article/pii/B9780123971791000129

[17] D. S. Faber and A. E. Pereda, "Two forms of electrical transmission between neurons," *Frontiers Mol. Neurosci.*, vol. 11, p. 427, Nov. 2018.

[18] D. L. Felten, M. K. O'Banion, and M. S. Maida, "1—Neurons and their properties," in *Netter's Atlas of Neuroscience*, 3rd ed., Amsterdam, The Netherlands: Elsevier, 2016, pp. 1–42. [Online]. Available: https://www.sciencedirect.com/science/article/pii/B9780323265119000011

[19] K. A. Ng, C. Yuan, A. Rusly, A.-T. Do, B. Zhao, S.-C. Liu, W. Y. X. Peh, X. Y. Thow, K. Voges, S. Lee, G. G. L. Gammad, K.-W. Leong, J. S. Ho, S. Bossi, G. Taverni, A. Cutrone, S.-C. Yen, and Y. P. Xu, "A wireless multi-channel peripheral nerve signal acquisition system-on-chip," *IEEE J. Solid-State Circuits*, vol. 54, no. 8, pp. 2266–2280, Aug. 2019.

[20] M. Asif, M. I. Tiwana, U. S. Khan, W. S. Qureshi, J. Iqbal, N. Rashid, and N. Naseer, "Advancements, trends and future prospects of lower limb prosthesis," *IEEE Access*, vol. 9, pp. 85956–85977, 2021.

[21] A. Akinin, A. Paul, J. Wang, A. Buccino, and G. Cauwenberghs, "Biopotential measurements and electrodes," in *Neural Engineering*, B. He, Ed., Cham, Switzerland: Springer, 2020, pp. 65–96, doi: 10.1007/978-3-030-43395-6_2.

[22] S. Behtaj, J. St John, J. K. Ekberg, and M. Rybachuk, "Neuron-fibrous scaffold interfaces in the peripheral nervous system: A perspective on the structural requirements," *Neural Regener. Res.*, vol. 17, no. 9, p. 1893, 2022.

[23] J. Lee, V. Leung, A.-H. Lee, J. Huang, P. Asbeck, P. P. Mercier, S. Shellhammer, L. Larson, F. Laiwalla, and A. Nurmikko, "Neural recording and stimulation using wireless networks of microimplants," *Nature Electron.*, vol. 4, no. 8, pp. 604–614, Aug. 2021, doi: 10.1038/s41928-021-00631-8.

[24] L. Yan, S. Liu, J. Wang, X. Ding, Y. Zhao, N. Gao, Z. Xia, M. Li, Q. Wei, O. V. Okoro, Y. Sun, L. Nie, A. Shavandi, G. Jiang, J. Chen, L. Fan, and Y. Weng, "Constructing nerve guidance conduit using dECM-doped conductive hydrogel to promote peripheral nerve regeneration," *Adv. Funct. Mater.*, vol. 34, no. 30, 2024, Art. no. 2402698.

[25] K.-I. Song, S. E. Park, S. Lee, H. Kim, S. H. Lee, and I. Youn, "Compact optical nerve cuff electrode for simultaneous neural activity monitoring and optogenetic stimulation of peripheral nerves," *Sci. Rep.*, vol. 8, no. 1, p. 15630, Oct. 2018, doi: 10.1038/s41598-018-33695-2.

[26] S. Sadrafshari, B. Metcalfe, N. Donaldson, N. Granger, J. Prager, and J. Taylor, "The design of a low noise, multi-channel recording system for use in implanted peripheral nerve interfaces," *Sensors*, vol. 22, no. 9, p. 3450, Apr. 2022.

[27] R. G. L. Koh, J. Zariffa, L. Jabban, S.-C. Yen, N. Donaldson, and B. W. Metcalfe, "Tutorial: A guide to techniques for analysing recordings from the peripheral nervous system," *J. Neural Eng.*, vol. 19, no. 4, Aug. 2022, Art. no. 042001, doi: 10.1088/1741-2552/ac7d74.

[28] E. H. Rijnbeek, N. Eleveld, and W. Olthuis, "Update on peripheral nerve electrodes for closed-loop neuroprosthetics," *Frontiers Neurosci.*, vol. 12, p. 350, May 2018, doi: 10.3389/fnins.2018.00350.

[29] M. Ortiz-Catalan, R. Brånemark, B. Håkansson, and J. Delbeke, "On the viability of implantable electrodes for the natural control of artificial limbs: Review and discussion," *Biomed. Eng. OnLine*, vol. 11, no. 1, p. 33, 2012.

[30] K. A. Yildiz, A. Y. Shin, and K. R. Kaufman, "Interfaces with the peripheral nervous system for the control of a neuroprosthetic limb: A review," *J. NeuroEng. Rehabil.*, vol. 17, no. 1, pp. 5–43, Dec. 2020.

[31] R. G. L. Koh, M. Balas, A. I. Nachman, and J. Zariffa, "Selective peripheral nerve recordings from nerve cuff electrodes using convolutional neural networks," *J. Neural Eng.*, vol. 17, no. 1, Jan. 2020, Art. no. 016042, doi: 10.1088/1741-2552/ab4ac4.

[32] J. G. Webster, "Biomedical instrumentation," in *Handbook of Research on Biomedical Engineering Education and Advanced Bioengineering Learning: Interdisciplinary Concepts*, Z. O. Abu-Faraj, Ed., Hershey, PA, USA: IGI Global, 2012, pp. 339–355, doi: 10.4018/978-1-4666-0122-2.ch008.

[33] R. Sahyouni, A. Mahmoodi, J. W. Chen, D. T. Chang, O. Moshtaghi, H. R. Djalilian, and H. W. Lin, "Interfacing with the nervous system: A review of current bioelectric technologies," *Neurosurgical Rev.*, vol. 42, no. 2, pp. 227–241, Jun. 2019, doi: 10.1007/s10143-017-0920-2.

[34] C. Eder, S. S. Zehra, M. Zamani, and A. Demosthenous, "Suitable compensation circuits for on-chip interference reduction in neural tripolar recordings," in *Proc. IEEE 20th Int. Conf. Electron., Circuits, Syst. (ICECS)*, Dec. 2013, pp. 241–244.

[35] C. E. Larson and E. Meng, "A review for the peripheral nerve interface designer," *J. Neurosci. Methods*, vol. 332, Feb. 2020, Art. no. 108523. [Online]. Available: https://www.sciencedirect.com/science/article/pii/S0165027019303802

[36] J.-U. Chu, K.-I. Song, S. Han, S. H. Lee, J. Kim, J. Y. Kang, D. Hwang, J.-K.-F. Suh, K. Choi, and I. Youn, "Improvement of signal-to-interference ratio and signal-to-noise ratio in nerve cuff electrode systems," *Physiolog. Meas.*, vol. 33, no. 6, pp. 943–967, Jun. 2012, doi: 10.1088/0967-3334/33/6/943.

[37] C. Pflaum, R. R. Riso, and G. Wiesspeiner, "Performance of alternative amplifier configurations for tripolar nerve cuff recorded ENG," in *Proc. 18th Annu. Int. Conf. IEEE Eng. Med. Biol. Soc.*, vol. 1, Oct. 1996, pp. 375–376.

[38] C. Eder and A. Demosthenous, "Electrical biosensors: Peripheral nerve sensors," in *Handbook of Biochips: Integrated Circuits and Systems for Biology and Medicine*, vol. 2015, M. Sawan, Ed., New York, NY, USA: Springer, 1007, pp. 1–21, doi: 10.1007/978-1-4614-6623-9_28-1.

[39] M. Sharma, A. Gardner, H. Strathman, D. Warren, J. Silver, and R. Walker, "Acquisition of neural action potentials using rapid multiplexing directly at the electrodes," *Micromachines*, vol. 9, no. 10, p. 477, Sep. 2018.

[40] J. E. B. Randles, "Kinetics of rapid electrode reactions," *Discuss. Faraday Soc.*, vol. 1, no. 1, pp. 11–19, 1947, doi: 10.1039/df9470100011.

[41] N. Jowett, R. E. Kearney, C. J. Knox, and T. A. Hadlock, "Toward the bionic face: A novel neuroprosthetic device paradigm for facial reanimation consisting of neural blockade and functional electrical stimulation," *Plastic Reconstructive Surg.*, vol. 143, no. 1, pp. 62e–76e, 2019.

[42] S. Askari, A. Presacco, R. Sahyouni, H. Djalilian, A. Shkel, and H. Lin, "Closed loop microfabricated facial reanimation device coupling EMG-driven facial nerve stimulation with a chronically implanted multichannel cuff electrode," in *Proc. 40th Annu. Int. Conf. IEEE Eng. Med. Biol. Soc. (EMBC)*, Jul. 2018, pp. 2206–2209.

[43] J. Li, X. Liu, W. Mao, T. Chen, and H. Yu, "Advances in neural recording and stimulation integrated circuits," *Frontiers Neurosci.*, vol. 15, Aug. 2021, Art. no. 663204.

[44] J. Chen, M. Tarkhan, H. Wu, F. H. Noshahr, J. Yang, and M. Sawan, "Recent trends and future prospects of neural recording circuits and systems: A tutorial brief," *IEEE Trans. Circuits Syst. II, Exp. Briefs*, vol. 69, no. 6, pp. 2654–2660, Jun. 2022.

[45] Y. Wang, X. Zhang, M. Liu, W. Pei, K. Wang, and H. Chen, "An implantable sacral nerve root recording and stimulation system for micturition function restoration," *IEICE Trans. Inf. Syst.*, vol. E97.D, no. 10, pp. 2790–2801, 2014.

[46] C. M. Lopez and X. Huang, "Circuits and architectures for neural recording interfaces," in *Biomedical Electronics, Noise Shaping ADCs, and Frequency References: Advances in Analog Circuit Design 2022*, P. Harpe, A. Baschirotto and K. A. A. Makinwa, Eds., Cham, Switzerland: Springer, 2023, pp. 45–57, doi: 10.1007/978-3-031-28912-5_3.

[47] A. Deshmukh, L. Brown, M. F. Barbe, A. S. Braverman, E. Tiwari, L. Hobson, S. Shunmugam, O. Armitage, E. Hewage, M. R. Ruggieri, and J. Morizio, "Fully implantable neural recording and stimulation interfaces: Peripheral nerve interface applications," *J. Neurosci. Methods*, vol. 333, Mar. 2020, Art. no. 108562. [Online]. Available: https://www.sciencedirect.com/science/article/pii/S0165027019304194

[48] M. ElAnsary, J. Xu, J. S. Filho, G. Dutta, L. Long, C. Tejeiro, A. Shoukry, C. Tang, E. Kilinc, J. Joshi, P. Sabetian, S. Unger, J. Zariffa, P. Yoo, and R. Genov, "Bidirectional peripheral nerve interface with 64 second-order opamp-less $\triangle\Sigma$ ADCs and fully integrated wireless power/data transmission," *IEEE J. Solid-State Circuits*, vol. 56, no. 11, pp. 3247–3262, Nov. 2021.

[49] Y. Shen, C. Yang, Y. Zhang, W. Wang, Y. Luo, C. Yu, K. Xu, G. Pan, and B. Zhao, "A battery-free neural-recording chip achieving 5.5 cm fully-implanted depth by galvanically-switching passive body channel communication," *IEEE J. Solid-State Circuits*, vol. 59, no. 8, pp. 2591–2603, Aug. 2024.

[50] M. Taghadosi, L. Albasha, N. A. Quadir, Y. A. Rahama, and N. Qaddoumi, "High efficiency energy harvesters in 65nm CMOS process for autonomous IoT sensor applications," *IEEE Access*, vol. 6, pp. 2397–2409, 2018.

[51] N. A. Quadir, L. Albasha, M. Taghadosi, N. Qaddoumi, and B. Hatahet, "Low-power implanted sensor for orthodontic bond failure diagnosis and detection," *IEEE Sensors J.*, vol. 18, no. 7, pp. 3003–3009, Apr. 2018.

[52] E. Donati and G. Valle, "Neuromorphic hardware for somatosensory neuroprostheses," *Nature Commun.*, vol. 15, no. 1, p. 556, Jan. 2024, doi: 10.1038/s41467-024-44723-3.

[53] Y. Tanabe, J. S. Ho, J. Liu, S.-Y. Liao, Z. Zhen, S. Hsu, C. Shuto, Z.-Y. Zhu, A. Ma, C. Vassos, P. Chen, H. F. Tse, and A. S. Y. Poon, "High-performance wireless powering for peripheral nerve neuromodulation systems," *PLoS ONE*, vol. 12, no. 10, Oct. 2017, Art. no. e0186698.

[54] K. Kansaku, "Neuroprosthetics in systems neuroscience and medicine," *Sci. Rep.*, vol. 11, no. 1, p. 5404, 2021, doi: 10.1038/s41598-021-85134-4.

[55] L. Chee, G. Valle, G. Preatoni, C. Basla, M. Marazzi, and S. Raspopovic, "Cognitive benefits of using non-invasive compared to implantable neural feedback," *Sci. Rep.*, vol. 12, no. 1, p. 16696, 2022, doi: 10.1038/s41598-022-21057-y.

[56] H. Y. Song, D. W. Shin, S. M. Jung, Y. Jeong, B. Jeong, and C. S. Park, "Feasibility study on transcutaneous auricular vagus nerve stimulation using millimeter waves," *Biomed. Phys. Eng. Exp.*, vol. 7, no. 6, Nov. 2021, Art. no. 065028, doi: 10.1088/2057-1976/ac2c54.

[57] R. Chataut, M. Nankya, and R. Akl, "6G Networks and the AI revolution-exploring technologies, applications, and emerging challenges," *Sensors*, vol. 24, no. 6, pp. 2790–2801, 2024.

[58] V. Pikov and P. H. Siegel, "Novel neural interface for modulation of neuronal activity based on millimeter wave exposure," in *Proc. IEEE/NIH Life Sci. Syst. Appl. Workshop (LiSSA)*, Apr. 2011, pp. 147–151.

[59] O. N. Ionescu, E. Franti, V. Carbunaru, C. Moldovan, S. Dinulescu, M. Ion, D. C. Dragomir, C. M. Mihailescu, I. Lascar, A. M. Oproiu, T. P. Neagu, R. Costea, M. Dascalu, M. D. Teleanu, G. Ionescu, and R. Teleanu, "System of implantable electrodes for neural signal acquisition and stimulation for wirelessly connected forearm prosthesis," *Biosensors*, vol. 14, no. 1, p. 31, Jan. 2024.

[60] N. A. Quadir, M. Taghadosi, L. Albasha, and N. Qaddoumi, "Design of self powered chip integrated humidity sensor," in *Proc. IEEE 59th Int. Midwest Symp. Circuits Syst. (MWSCAS)*, Oct. 2016, pp. 1–4.

[61] H. Zonghao, W. Zhigong, L. Xiaoying, L. Wenyuan, S. Xiaoyan, Z. Xintai, X. Shushan, P. Haixian, and Z. Cunliang, "Design and experiment of a neural signal detection using a FES driving system," in *Proc. Annu. Int. Conf. IEEE Eng. Med. Biol.*, Aug. 2010, pp. 1523–1526.

[62] A. Shon, J.-U. Chu, J. Jung, H. Kim, and I. Youn, "An implantable wireless neural interface system for simultaneous recording and stimulation of peripheral nerve with a single cuff electrode," *Sensors*, vol. 18, no. 1, p. 1, Dec. 2017, doi: 10.3390/s18010001.

[63] C. Veraart, C. Raftopoulos, J. T. Mortimer, J. Delbeke, D. Pins, G. Michaux, A. Vanlierde, S. Parrini, and M.-C. Wanet-Defalque, "Visual sensations produced by optic nerve stimulation using an implanted self-sizing spiral cuff electrode," *Brain Res.*, vol. 813, no. 1, pp. 181–186, Nov. 1998. [Online]. Available: https://www.sciencedirect.com/science/article/pii/S0006899398009779

[64] N. Brill, K. Polasek, E. Oby, C. Ethier, L. Miller, and D. Tyler, "Nerve cuff stimulation and the effect of fascicular organization for hand grasp in nonhuman primates," in *Proc. Annu. Int. Conf. IEEE Eng. Med. Biol. Soc.*, Sep. 2009, pp. 1557–1560.

[65] R. Sahyouni, J. Bhatt, H. R. Djalilian, W. C. Tang, J. C. Middlebrooks, and H. W. Lin, "Selective stimulation of facial muscles with a penetrating electrode array in the feline model," *Laryngoscope*, vol. 127, no. 2, pp. 460–465, Feb. 2017.

[66] N. B. Langhals, M. G. Urbanchek, A. Ray, and M. J. Brenner, "Update in facial nerve paralysis: Tissue engineering and new technologies," *Curr. Opin. Otolaryngol. Head Neck Surg.*, vol. 22, no. 4, pp. 291–299, 2014.

[67] S. Oh, J. Jekal, J. Liu, J. Kim, J. Park, T. Lee, and K. Jang, "Bioelectronic implantable devices for physiological signal recording and closed-loop neuromodulation," *Adv. Funct. Mater.*, vol. 34, no. 28, Jul. 2024, Art. no. 2403562.

[68] J. Cho, G. Seong, Y. Chang, and C. Kim, "Energy-efficient integrated circuit solutions toward miniaturized closed-loop neural interface systems," *Frontiers Neurosci.*, vol. 15, May 2021, Art. no. 667447.

[69] D. Loi, C. Carboni, G. Angius, G. N. Angotzi, M. Barbaro, L. Raffo, S. Raspopovic, and X. Navarro, "Peripheral neural activity recording and stimulation system," *IEEE Trans. Biomed. Circuits Syst.*, vol. 5, no. 4, pp. 368–379, Aug. 2011.

[70] O. Phokaewvarangkul, A. Balachandar, and A. Fasano, "Closed-loop systems," in *Handbook of Digital Technologies in Movement Disorders*, R. Bhidayasiri and W. Maetzle, Eds., New York, NY, USA: Academic, 2024, ch. 17, pp. 269–284. [Online]. Available: https://www.sciencedirect.com/science/article/pii/B9780323994941000022

[71] E. L. O'Callaghan, F. D. McBryde, A. E. Burchell, L. E. K. Ratcliffe, L. Nicolae, I. Gillbe, D. Carr, E. C. Hart, A. K. Nightingale, N. K. Patel, and J. F. R. Paton, "Deep brain stimulation for the treatment of resistant hypertension," *Current Hypertension Rep.*, vol. 16, no. 11, p. 493, Nov. 2014, doi: 10.1007/s11906-014-0493-1.

[72] A. Shen, R. Li, Y. Li, J. Guo, J. Wang, and X. Sui, "A system of real-time neural recording and stimulation and its potential application in blood pressure modulation," *Frontiers Med. Technol.*, vol. 4, Aug. 2022, Art. no. 941686.

[73] M. Shoaran, "Next-generation closed-loop neural interfaces: Circuit and AI-driven innovations," *IEEE Solid StateCircuits Mag.*, vol. 15, no. 4, pp. 41–49, Nov. 2023.

[74] K. A. Ng, E. Greenwald, Y. P. Xu, and N. V. Thakor, "Implantable neurotechnologies: A review of integrated circuit neural amplifiers," *Med. Biol. Eng. Comput.*, vol. 54, no. 1, pp. 45–62, Jan. 2016.

[75] B. Gosselin, "Recent advances in neural recording microsystems," *Sensors*, vol. 11, no. 5, pp. 4572–4597, Apr. 2011.

[76] K. A. Ng and Y. P. Xu, "A compact, low input capacitance neural recording amplifier," *IEEE Trans. Biomed. Circuits Syst.*, vol. 7, no. 5, pp. 610–620, Oct. 2013.

[77] K. Naderi, E. H. T. Shad, M. Molinas, A. Heidari, and T. Ytterdal, "A very low SEF neural amplifier by utilizing a high swing current-reuse amplifier," in *Proc. 35th Conf. Design Circuits Integr. Syst. (DCIS)*, Nov. 2020, pp. 1–4.

[78] U. Kumari and R. Yadav, "A review about analysis and design methodology of two-stage operational transconductance amplifier (OTA)," in *Proc. Int. Conf. Data Sci. Appl.*, 2023, pp. 849–860.

[79] J. Liu and R. M. Walker, "A compact, low-noise, chopped front-end for peripheral nerve recording in 180 nm CMOS," in *Proc. IEEE Biomed. Circuits Syst. Conf. (BioCAS)*, Oct. 2018, pp. 1–4.

[80] Y. M. Dweiri, T. Eggers, G. McCallum, and D. M. Durand, "Ultra-low noise miniaturized neural amplifier with hardware averaging," *J. Neural Eng.*, vol. 12, no. 4, Aug. 2015, Art. no. 046024, doi: 10.1088/1741-2560/12/4/046024.

[81] A. Demosthenous, I. Pachnis, D. Jiang, and N. Donaldson, "An integrated amplifier with passive neutralization of myoelectric interference from neural recording tripoles," *IEEE Sensors J.*, vol. 13, no. 9, pp. 3236–3248, Sep. 2013.

[82] S. Simmich, A. Bahr, and R. Rieger, "Noise efficient integrated amplifier designs for biomedical applications," *Electronics*, vol. 10, no. 13, p. 1522, Jun. 2021.

[83] F. Hashemi Noshahr, M. Nabavi, and M. Sawan, "Multi-channel neural recording implants: A review," *Sensors*, vol. 20, no. 3, p. 904, Feb. 2020.

[84] M. Zhang, Z. Tang, X. Liu, and J. Van der Spiegel, "Electronic neural interfaces," *Nature Electron.*, vol. 3, no. 4, pp. 191–200, Apr. 2020, doi: 10.1038/s41928-020-0390-3.

[85] L. Wang, Y. Suo, J. Wang, X. Wang, K. Xue, J. An, X. Sun, Q. Chen, X. Tang, Y. Zhao, B. Ji, and J. Liu, "High-density implantable neural electrodes and chips for massive neural recordings," *Brain-X*, vol. 2, no. 2, p. e65, Jun. 2024, doi: 10.1002/brx2.65.

[86] V. Paggi, F. Fallegger, L. Serex, O. Rizzo, K. Galan, A. Giannotti, I. Furfaro, C. Zinno, F. Bernini, S. Micera, and S. P. Lacour, "A soft, scalable and adaptable multi-contact cuff electrode for targeted peripheral nerve modulation," *Bioelectronic Med.*, vol. 10, no. 1, p. 6, Feb. 2024, doi: 10.1186/s42234-023-00137-y.

[87] R. Chen, A. Canales, and P. Anikeeva, "Neural recording and modulation technologies," *Nat. Rev. Mater.*, vol. 2, p. 16093, Jan. 1038, doi: 10.1038/natrevmats.2016.93.

MALAK MNEIMNEH received the B.Eng. degree in electronics engineering emphasis on biomedical engineering from Lebanese International University. She is currently pursuing the master's degree in biomedical engineering with American University of Sharjah. Her research interests include neural amplifiers, sensors, and nerve signal detection.

NASIR QUADIR received the B.Tech. degree in electronics and communication engineering from Jamia Millia Islamia University, New Delhi, India, in 1998, the M.Sc. degree in electronics engineering from Universiti Sains Malaysia, in 2001, and the Ph.D. degree in electrical engineering from the University College Cork, Ireland, in 2014.

From 2001 to 2010, he was with Sires Labs Sdn. Bhd., Malaysia, designing and developing chipsets for automotive applications. From 2013 to 2016, he was an SRC Postdoctoral Fellow with American University of Sharjah, United Arab Emirates. During that time, his research was focused on developing a biomedical humidity-based CMOS sensor for orthodontic applications. He joined the CMR Institute of Technology as an Associate Professor, in 2017. He is currently involved in research on developing sensors for the IoT with American University of Sharjah.

LUTFI ALBASHA (Senior Member, IEEE) received the B.Eng. and Ph.D. degrees in electronic and electrical engineering from the University of Leeds, Leeds, U.K., in 1990 and 1995, respectively.

He joined Sony Corporation, in 1997, and worked on commercial radio-frequency integrated circuit (RFIC) chip products for mobile handsets. In 2000, he joined Filtronic Semiconductors as a Senior Principal Engineer and created and managed an integrated circuit design team. The team supported the company foundry design enablement for mass production and taped out its first commercial chips. This has become a very successful business in Europe's largest MMIC foundry. He returned to Sony as a Lead Principal Engineer, where he was involved in highly integrated RFCMOS and BiCMOS transceivers for cellular and DTV applications. He joined the American University of Sharjah, Sharjah, United Arab Emirates, where he progressed to Full Professor rank. His current research interests include energy harvesting, portable radars, wireless power transfer, wearable and implantable devices, power amplifier design, and integrated radar transceivers. He has received several outstanding recognition awards from industry and academia. He served for three terms as the Chairperson for the UAE Chapter of the IEEE Solid-State Circuits Society. He is an Associate Editor of *IET Microwaves, Antenna and Propagation* journal.